A Neural-Counting Model Based on Physiological Characteristics of the Peripheral Auditory System. IV. Application to Response of Individual Neural Fibers

GERARD LACHS, SENIOR MEMBER, IEEE, ROSALIE A. SAIA, MEMBER, IEEE, AND MALVIN C. TEICH, SENIOR MEMBER, IEEE

Abstract—**An energy-based neural-counting model, incorporating refractoriness and spread of excitation, has recently been applied to intensity discrimination and loudness estimation for a variety of acoustic stimuli. In this model, refractoriness was the sole means of achieving the saturation effect of the afferent fiber's response. Though refractoriness (or an effect like it) should be included in a proper Poisson-based model to produce a neural count variance less than the count mean (in accordance with experiment), there is a strong additional saturation effect associated with the response of the receptor. This earlier model is now extended to incorporate the effects of receptor saturation and spontaneous neural activity. In this paper the behavior of individual neural channels is investigated. Theoretical firing-rate curves are obtained as a function of stimulus level and frequency (isointensity contours). These are found to be in good agreement with neurophysiological data. It is shown that it is possible to fit human psychophysical tuning curves with a double-tuned linear filter, by judicious choice of the tuning parameter Q.**

Manuscript received June 14, 1983. This work was supported by the National Science Foundation under Grant BNS80-21140.

G. Lachs is with the Department of Electrical Engineering, Pennsylvania State University, University Park, PA 16802.

R. A. Saia was with the Department of Electrical Engineering, Pennsylvania State University, University Park, PA 16802. She is now with the TRW, 1 Space Park, Redondo Beach, CA 90278.

M. C. Teich is with the Department of Electrical Engineering, Columbia University, 520 W. 120 Street, New York, NY 10027.

I. Introduction

THIS is the fourth in a series of papers demonstrating the effectiveness of a mathematical model for predicting certain characteristics of the auditory system. The goal of this work is the development of a useful general model, founded on a number of elemental components, and possessing parametric values in accordance with observed values. In [10, part I it was demonstrated that an energy-based neural-counting model incorporating refractoriness and spread of excitation satisfactorily described the results of pure-tone intensity discrimination experiments. In [4] (Part II) it was shown that the identical linear filter refractoriness model (LFRM) also provided sensible results for pure-tone loudness estimation experiments at all stimulus levels. In [11] (Part III) this model is considered in the context of variable-bandwidth noise stimuli. The specific model discussed in [10], [4], and [11] did not account for

0018-9472/83/0900-0964$01.00

the details of the receptor response, assuming it to be linearly proportional to the driving stimulus energy. In essence, it utilized the refractoriness modifications of the Poisson process as the sole means of mathematically realizing the known saturation of the inner-ear response. One of the most obvious discrepancies between experiment and the LFRM arises in the value for the mean-to-variance ratio of the number of neural events observed on single fibers of the VIIIth nerve. Experimentally, this quantity tends toward a fixed limit with increasing stimulus level; however, when calculated on the basis of the LFRM, this ratio increases without bound as the stimulus energy increases. This discrepancy is eliminated in the work presented here.

We have extended the model of Parts I, II, and III ([10], [4], and [11]) to include the effects of receptor saturation and spontaneous neural activity in the primary afferent fibers. This is accomplished by incorporating a receptor saturation function that maps the stimulus energy in each channel into a driving rate for a Poisson process. Through this function, we incorporate the spontaneous activity and saturating response observed in single auditory fibers, and achieve a constant count mean-to-variance ratio for large stimulus energies. It will be shown that such a function, when used in conjunction with the tuned-filter response and dead-time modifications discussed in [10], [4], and [11], provides a good fit to related neurophysiological phenomena. The LFRM, as modified to include the effects of receptor response, will be referred to as the extended linear filter refractoriness model (ELFRM). A preliminary account of this work was presented at the Annual Meeting of the Acoustical Society of America in Chicago [3].

Two different receptor saturation functions were studied in detail. The first is based on a theoretical argument put forth by Zwislocki [15]. The form of this equation is basically exponential, and exhibits a hard saturating response for sufficiently strong stimuli. The second saturation function was designed to produce Weber's law, and a fixed mean-to-variance ratio for large stimulus levels, in each channel. The basis of this function is the natural logarithm, which exhibits a softer saturation.

In this paper, we consider the response of the individual neural channels comprising the ELFRM. We compare the predictions of the ELFRM with various neurophysiological and psychophysical tuning experiments. The calculated mean-to-variance ratio with dead-time modification included, as predicted by the ELFRM, is designed to be comparable with neurophysiological data [9]. Data for neural firing rate, as a function of stimulus intensity, as well as neural isointensity contours, are then modeled. All of these tasks make use of the ELFRM on a single channel basis, and are useful in determining an acceptable range for each of the key parameters. Finally, we show that the sharp tuning characteristics associated with psychophysical masking in the human auditory system can be fit by an appropriate choice of the parameters for the linear filter employed in the model. These values turn out to be sensible.

In a companion paper [12], we will discuss the application of the ELFRM to psychophysical intensity discrimination, loudness estimation, and loudness summation. That work will rely on the sum of the responses of all neural channels, and the parameter values obtained by the modeling procedure used in this paper will be used to model the psychophysical phenomena examined in [12].

In Section II, we introduce the extended model and discuss its mathematical characteristics. Comparisons of the calculated results with neurophysiological and psychophysical data will be described in Section III. Section IV contains a discussion of the results and conclusions.

II. Detection Model

A. Discussion of the Model

The extended linear filter refractoriness model (ELFRM) is based on the LFRM discussed in [10], [4], and [11] and is illustrated in Fig. 1. The modeling procedures discussed in this paper are for single channel responses. The input signal is assumed to excite the inner ear; we consider the transmission of the stimulus through the outer and middle ears to be essentially linear filtering. Though the presence of harmonics and combination tones is important for some paradigms, we do not consider them here. The modeling of the inner auditory system is both difficult and challenging. In particular, the dynamics of cochlear and receptor motion are not very well understood, and there are many nonlinear effects associated with these elements. Our basic construct for this part of the auditory system, as described below, consists of a linear filter followed by a nonlinear element. This is, of course, a gross idealization. But it captures the behavior of the inner ear, as it applies to the paradigms we consider, in a simple way.

The input is presented to a series of tuned asymmetric linear filters, each with its own characteristic or best frequency f_o. It is assumed that all fibers maximally sensitive to a particular frequency are represented as a single linear filter and comprise a single channel. We consider a continuum of such channels, across the range of audible frequencies. The strength of the stimulus in any particular channel is dependent upon the energy response of that channel's multiple-tuned (N-tuned or $2N$-pole) linear filter to the frequency(s) of stimulation f_T and is given by

$$E_o = \frac{E_i}{\left[1 + Q^2(f_T/f_o - f_o/f_T)^2\right]^N}. \tag{1}$$

Here E_o and E_i are the output and input energies of the filter, respectively, f_o is the best frequency of the neural channel, and Q is a tuning parameter (which is equal to the ratio of the best frequency to the 3-dB bandwidth for a single-tuned filter ($N = 1$)). Unless otherwise stated, $N = 2$ is employed for $f_T \leq f_o$ and $N = 4$ is employed for $f_T > f_o$, thereby incorporating the asymmetric frequency–response characteristics of the neural channels. The output of the filter is fed into a memoryless receptor saturation function (discussed in Section II-B) which, in turn, feeds an ideal

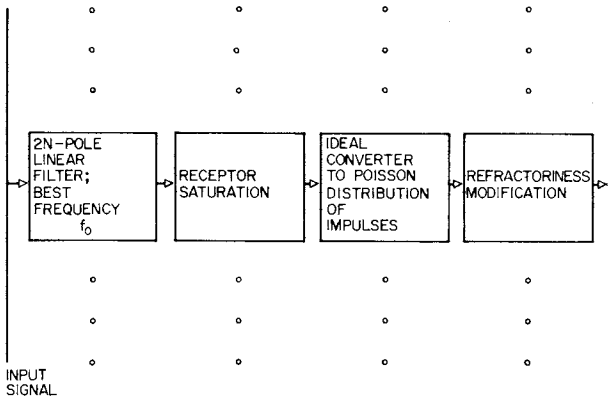

Fig. 1. Block diagram of the extended linear filter refractoriness model (ELFRM).

Poisson converter. The proportionality constant A that appears in [10, eq. (1)] is absorbed in the constant E_R (see Section II-B).

Based on the relative insensitivity of the neural *counting* statistics on characteristic frequency [9], we do not treat phase locking as a separate phenomenon. Rather, we consider the underlying neural count n for each channel to be a Poisson random variable driven by the filtered saturated stimulus energy. In this case

$$\bar{n}_u = \sigma_u^2, \tag{2}$$

where $\bar{n}_u$ and σ_u^2 are the (unmodified) count mean and variance, respectively, before modification by dead time (refractoriness).

The refractoriness modification is the final stage in the mathematical model for each individual channel, as shown in Fig. 1. We account for the dead time inherent in the system through the well-known formulas for an underlying Poisson process [10], [13]:

$$\bar{n}_c(f_o) = \frac{\bar{n}_u(f_o)}{1 + (\tau/T)\bar{n}_u(f_o)} \tag{3}$$

and

$$\sigma_c^2(f_o) = \frac{\bar{n}_u(f_o)}{[1 + (\tau/T)\bar{n}_u(f_o)]^3}, \tag{4}$$

where $\bar{n}_c(f_o)$ and $\sigma_c^2(f_o)$ are the corrected (modified) count mean and variance, respectively, $\bar{n}_u(f_o)$ is the unmodified mean count, τ is the nonparalyzable dead-time, and T is the counting time. In the LFRM discussed in [10], [4], and [11], the dead-time modifications were the sole means of mathematically achieving the saturation of the neural response. In the ELFRM, on the other hand, the effects of receptor saturation are explicitly defined. By separately considering saturation and dead-time effects, we are able to study the relative significance of each on the response of our model auditory system.

For many psychophysical tasks, the overall number of neural impulses on a collection of parallel channels, observed in a fixed but unspecified counting time T, appears to be a sufficient statistic. This aspect of the model presented in Fig. 1 will be discussed further in [12].

B. Receptor Saturation Function

As previously indicated, two distinct functional forms for the receptor saturation function were investigated. The first form [15] is given by

$$\bar{n}_u(f_o) = TR_M\left\{1 - \exp\left[\frac{-R_o}{R_M}\left(1 + \frac{E_o}{E_R}\right)^{\theta}\right]\right\}, \tag{5}$$

where R_M is defined as the hypothetical maximum response rate in spikes/s (before refractoriness modification) on a single neural fiber, R_o is the spontaneous discharge rate in spikes/s (which is assumed to be unaffected by the dead-time processes), E_R is a reference level that governs the channel threshold, and θ is a parameter that controls the maximum slope of the response (taken to be 0.5 throughout this paper).

The second saturation function that we have investigated is described by the expression

$$\bar{n}_u(f_o) = T\left\{R_o + \frac{\alpha(R_m - R_o)\ln(1 + E_o/E_R)}{1 + \alpha\left(\frac{R_m - R_o}{R_M - R_o}\right)\ln(1 + E_o/E_R)}\right\}, \tag{6}$$

where α determines the maximum slope of the response (analogous to θ in (5)). The quantities R_o, R_M, and E_R are defined above, and the quantity R_m is the maximum observed firing rate in spikes/s after refractoriness modification. This function is discussed in substantial detail in the Appendix. The stimulus intensity or energy E_o, defined in both (5) and (6), is given by (1). Both functions introduce spontaneous and maximum response rates of single auditory fibers and allow for the introduction of a nonlinear receptor (hair cell) response.

III. Application of the ELFRM to Neurophysiological and Psychophysical Data

In Section III-A, we compare the mean-to-variance ratio of the count predicted by the ELFRM with observed neurophysiological values. In Section III-B, we compare the predicted mean response of single channels of the ELFRM with the observed response of single neural fibers. In particular, we examine the dynamic range and the response rate, as a function of the stimulus energy and frequency. The neurophysiological data are drawn from Kiang [2] and from Rose *et al.* [8]. In Section III-C we discuss the procedure used for modeling human psychophysical tuning curves, and compare the results with those of Johnson-Davies and Patterson [1]. The data fitting procedures discussed in this section provide a representative range for the parameters of the ELFRM model to be used in other studies. Though the derived values are appropriate for the auditory system of cats or squirrel monkeys, it will be demonstrated in [12] that these parameters are also suitable for fitting a broad variety of psychophysical data obtained from humans.

A. Mean-to-Variance Ratio of the Neural Count

We begin with a discussion of the count mean-to-variance ratio γ as a function of the stimulus intensity, for typical primary afferent fibers. Neurophysiological experiments in the cat demonstrate that this ratio approaches a relatively constant value, between 1 and 2 for $T = 50$ ms, as the stimulus energy is increased [9]. This value appears to be relatively independent of the characteristic frequency of the fiber. The mean-to-variance ratio γ predicted by the ELFRM is obtained from (3) and (4):

$$\gamma = [1 + (\tau/T)\bar{n}_u(f_o)]^2. \tag{7}$$

Here, $\bar{n}_u(f_o)/T$ is the uncorrected mean firing rate, per fiber, which in our case is determined from either (5) or (6).

The LFRM model of [10], [4], and [11] assumed $\bar{n}_u(f_o)$ to be linearly proportional to the stimulus energy, in which case

$$\gamma_{\text{LFRM}} = [1 + (\tau/T)(aE_o)]^2, \tag{8}$$

where a is a constant. It is clear that γ_{LFRM}, represented in (8), increases without bound as the stimulus energy gets larger. The saturating rate function in the ELFRM eliminates this disagreement with experiment. If, for example, the saturation function of (5) is used in (7), for large stimulus intensities the calculated mean-to-variance ratio approaches

$$\gamma_{\text{exp}} \simeq [1 + \tau R_M]^2, \tag{9}$$

so that

$$\tau = (\sqrt{\gamma} - 1)/R_M. \tag{10}$$

Thus, γ may be found from τ and R_M or, conversely, the dead time τ may be found from γ and R_M. Furthermore, $R_M = \sqrt{\gamma} R_m$. It is shown in the Appendix that identical results are obtained for the logarithmic saturation function (see (27)–(29)).

We next consider the mean response of single afferent units to various stimulus frequencies and intensities.

B. Single-Channel Mean Response

Perhaps the simplest observation of neural activity is the mean firing rate as a function of stimulus intensity (for a fixed stimulus frequency). In a typical experiment, the neural unit is stimulated at its characteristic (or best) frequency. By varying the stimulus intensity, it is possible to determine: a) the spontaneous response rate of the neural unit, b) the dynamic range (response range) of the unit, and c) the maximum rate of response elicited.

Evaluation of the mean response rate for the ELFRM begins with the tuned-filter response represented in (1). For the frequency of stimulation equal to the characteristic frequency, the denominator of (1) becomes unity for all values of Q and N, so that

$$E_o = E_i. \tag{11}$$

We wish to evaluate the modified mean $\bar{n}_c(f_o)$, utilizing (3) and either (5) or (6). Figs. 2(a) and (b) show the best fit to the experimental mean firing rate function versus intensity level for a particular unit (data adapted from [2] as replotted in [15]), for the exponential and logarithmic receptor saturation functions, respectively. The values used for the parameters of each function are reported in the figure caption.

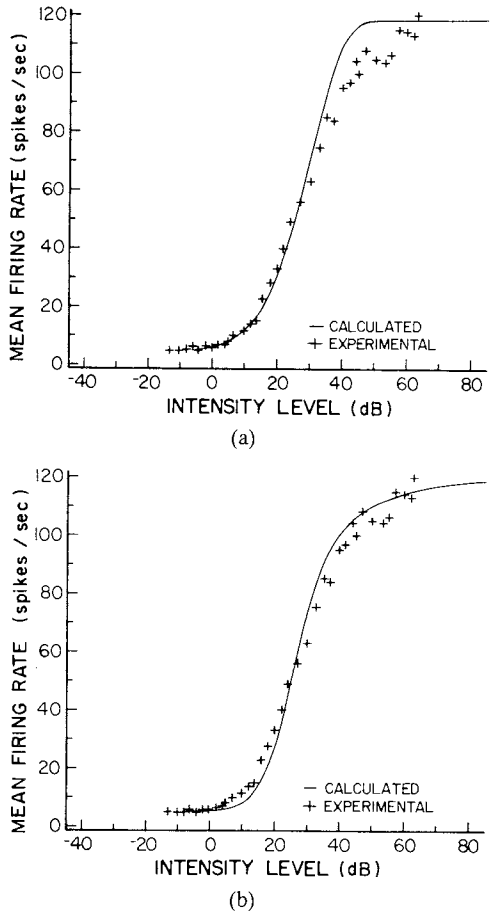

Fig. 2. Mean firing rate for a single afferent fiber, in response to a tone of frequency equal to the fiber's characteristic frequency (CF = 5.83 kHz), as a function of the stimulus intensity (dB). Experimental data (+) reported by Kiang [15] and adapted by Zwislocki [2]. ELFRM results (solid curves) for (a) exponential receptor saturation function and (b) logarithmic receptor saturation function. Key parameters for each case are: (a) $R_o = 5.0$, $R_M = 147$, $E_R = 2.0$, $\theta = 0.5$, $\gamma = 1.5$; (b) $R_o = 5.0$, $R_m = 120.0$, $E_R = 600.0$, $\alpha = 1.4$, $\gamma = 1.5$.

We first discuss the parameters for Fig. 2(a). The value of θ was chosen, as indicated, to be 0.5. This was determined by varying the magnitude of θ to determine its effect on the rate function. We found that its value primarily influenced the slope of the response in the curve's central region. Lower values of θ produced a shallower response; higher values decreased the dynamic range of the theoretical unit. The value $\theta = 0.5$ was also suggested by Zwislocki [15]. This parameter remains constant throughout the remaining fitting procedures. The magnitude of R_o, the spontaneous firing rate, was taken directly from the experimental data. The value of R_M was chosen to achieve the maximum response rate, indicated by the experimental data, after the dead-time correction has been made. The quantity γ was chosen to be 1.5 throughout. E_R is, perhaps,

the only true free parameter in this modeling task. Its influence is to shift the calculated curve horizontally; thus its magnitude was chosen to align the calculated and experimental data.

In Fig. 2(b) we directly assign the experimental values for the spontaneous and maximum response rates to R_o and R_m, respectively. We insert the observed maximum firing rate in the case of the logarithmic saturation function, since the effects of refractoriness are already incorporated into its form (see Appendix). The counterpart of θ is α, which affects the dynamic range of the theoretical neural unit. The best fit for the particular unit illustrated requires $\alpha = 1.4$. Typical values for this parameter, used in other modeling procedures, lie between 0.5 and 1.5. Again, $\gamma = 1.5$. The reference level parameter E_R was chosen in the same manner as described above, i.e., to align the calculated response curve with the experimental data.

Comparing Figs. 2(a) and (b) demonstrates that the exponential function exhibits a harder saturation than the logarithmic function. Both provide good fits to this particular set of neurophysiological data; however, these results are not representative of all auditory units. Indeed Liberman [5], [6] has shown that there are classes of auditory units, exhibiting both low and high spontaneous firing rates. In this paper we have explicitly modeled the response of several low spontaneous units; in [12], we also discuss the effects of high spontaneous response rates on psychophysical modeling.

A pertinent physiological characteristic of the auditory system is the response of a neural unit to frequencies away from the characteristic frequency (CF). This is evident in the neural firing characteristics recorded by Rose, Hind, Anderson, and Brugge [8], and is incorporated into the ELFRM through the multiple-tuned linear-filter response function. The experimental data collected in [8] was obtained by measuring the mean firing rate of individual VIIIth-nerve auditory neurons excited by pure-tone stimuli of given intensity level and variable frequency (isointensity contours). In general, when presented on a linear–linear plot, these contours display rather narrow response widths for low stimulus intensities, which broaden significantly as the stimulus level increases. Spontaneous and maximum firing rates vary with each unit. The ELFRM model was implemented by evaluating the mean count rate of a single channel, including refractoriness modifications. This calculation makes use of (1), (3), and (5) or (6).

Figs. 3(a) and (b) represent calculated isointensity contours of a theoretical auditory nerve unit most sensitive to 2100 Hz. These are the predicted neural-firing characteristics, using the exponential and logarithmic saturation functions, respectively. They may be compared with the contours shown in Fig. 3(c), which are the experimental results obtained by Rose *et al.* [8]. The parameter values used to fit these data are listed in Table I. Note, once again, that the value of R_m used to produce the curves in Fig. 3(b) is that of the observed maximum response rate, as shown in Fig. 3(c). However, the value of R_M used with the exponential function, Fig. 3(a), is larger than R_m (see (29)). This is

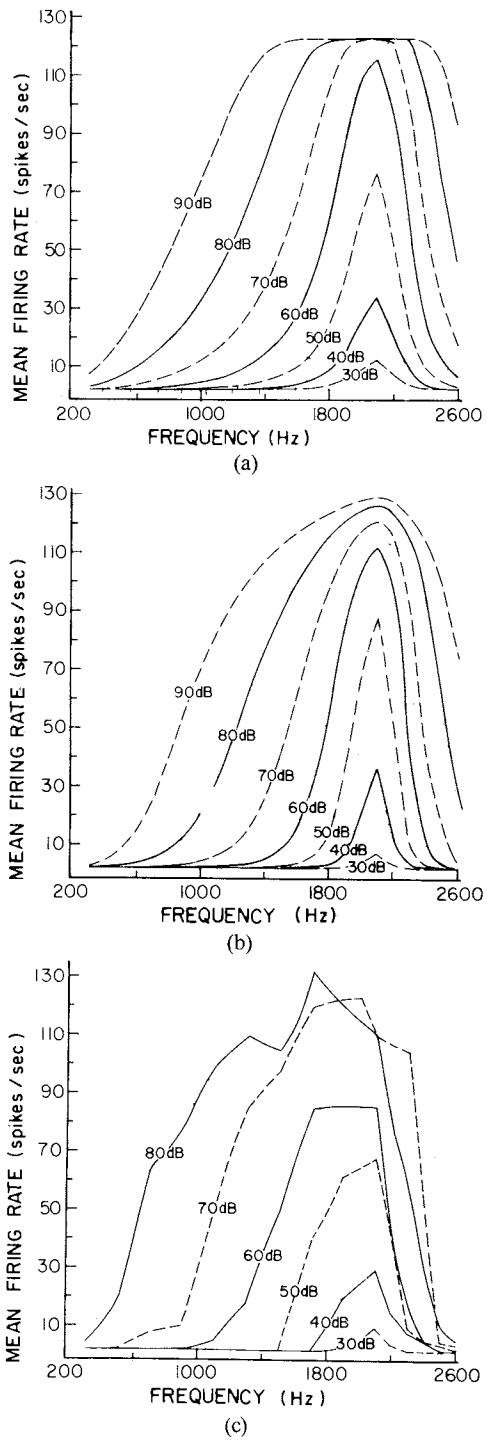

Fig. 3. Mean response of a single afferent fiber to a tone of variable frequency and intensity. (a) The ELFRM results using the exponential receptor saturation function. (b) Results were calculated using the logarithmic function. (c) Data collected by Rose *et al.* [8] are shown for a fiber with a characteristic frequency of 2100 Hz. (Pertinent parameter values are listed in Table I.)

because the logarithmic form was designed with the dead time in mind, whereas the exponential form was not. The parameters N and Q are brought into play by the tuned linear-filter response. The larger the value of Q, the sharper the tuning. It will be shown in Section III-C that values of $Q \sim 5$ also provide suitable fits to the psychophysical tuning curves. As in [10], [4], and [11], the pole-pair para-

TABLE I
PARAMETERS FOR THE ELFRM THEORETICAL ISOINTENSITY CONTOURS[a]

Functional Form of Saturation Function	Parameters[1]	CF = 2100 Hz [Figs. 3(a), 3(b)]	CF = 4100 Hz [Figs. 4(a), 4(b)]
Exponential	R_M (Spikes/s)[2]	159	128
	Q (Single-Tuned Value)	7.7	7.7
	E_R (Stimulus Units)	5.0	5.0×10^3
	τ (ms)	1.42	1.75
Logarithmic	R_m (Spikes/s)[2]	130	105
	Q (Single-Tuned Value)	7.7	7.7
	E_R (Stimulus Units)	6.0×10^3	7.5×10^5
	τ (ms)	1.42	1.75

[a]The following parameters have been given the same values for all cases: $R_o = 2.0$ spikes/s; $\gamma = 1.5$; $\theta = 0.5$, applicable only in exponential case; $\alpha = 1.4$, applicable only in logarithmic case; $N = 2$ $(f_T \leq f_o)$, $N = 4(f_T > f_o)$.
[2]See (29) for relation between R_M and R_m.

meter N was taken to be 2 for $f_T \leq f_o$ and 4 for $f_T > f_o$. Again, the value of E_R was chosen to align the threshold levels of the experimental and calculated data.

To demonstrate the robustness of the ELFRM, as well as the suitability of the functional relationships investigated, the isointensity contours for a fiber with a CF of 4100 Hz have been generated using the same approach. Figs. 4 (a), (b), and (c) present contours obtained using the exponential saturation function, the logarithmic saturation function, and the experimental data (Rose *et al.* [8]), respectively. The values for the various parameters used to produce each set of curves are comparable with those used for Fig. 3 (see Table I).

The data that we have dealt with has, to this point, been neurophysiological in nature. An important question is how suitably the ELFRM predicts psychophysical phenomena, and whether the (neurophysiological) parameter values provided in Table I are applicable to such (psychophysical) data. In the next section, we discuss the application of the ELFRM to psychophysical tuning curves, which are a manifestation of the auditory system's tuning mechanisms. Other psychological paradigms will be discussed in [12].

C. Human Psychophysical Tuning Curves

The psychophysical counterpart of the neural tuning curve is the psychophysical tuning curve. These are typically obtained [14] by presenting a human observer with a probe tone, generally of fixed frequency and level, and then measuring the power necessary for a masking tone to just mask the probe as a function of the frequency of the masker. As in most experimental situations, there are numerous variations on this theme. There are, for example, noise maskers, and forward, simultaneous, and backward masking paradigms.

Psychophysical tuning curves are usually obtained in the neighborhood of threshold, which may permit the approximation that only a small number of neural fibers are active, and that saturation and refractoriness effects may be neglected. Considering only a single channel at the probe frequency, then, we calculate the masker level required for masking by means of the relation

$$E_o/E_i = \left[1 + Q^2\left(f_M/f_p - f_p/f_M\right)^2\right]^{-rN}. \quad (12)$$

The masker level (in dB) is then given by $-10\log(E_o/E_i)$. This expression is similar to that provided in (1), except that now f_M is the masker frequency, f_p is the probe frequency, and Q is the (single-tuned) 3-dB tuning parameter. The factor r introduces the asymmetric behavior of the auditory filter.

The data depicted in Fig. 5 (open squares) were collected under a simultaneous masking paradigm [1], using a sinusoidal probe tone and a narrowband noise masker. In the ELFRM calculations, for simplicity, the narrowband noise was assumed to be a pure sinusoid of frequency equal to the center frequency of the masking noise (solid curve). The parameter values listed in the figure caption ($N = 2/N = 4$, $Q = 8.6$) are those used to produce the calculated results. Observe that we are able to fit the data using the $N = 2/N = 4$ model employed previously, and in [10], [4], and [11]. It is important to note that the $6N$ dB/octave roll-off associated with an N-tuned circuit applies only in the tails of the transfer function. By appropriate choice of the parameter Q, we are able to achieve the 160 dB/octave roll-off on the high-frequency side, and the 120 dB/octave roll-off on the low-frequency side reported by Johnson-Davies and Patterson [1] in the vicinity of resonance. Note also that the choice of Q is comparable to that used in the neurophysiological model discussed earlier.

This paper is principally based on the physiological response characteristics of peripheral auditory fibers. We have considered the fits to psychophysical data primarily as an indication that our results are applicable to humans as well as to cats and squirrel monkeys. We expect that the ELFRM would reproduce human neurophysiological tuning curves, with an appropriate choice of Q, were they available.

IV. DISCUSSION AND CONCLUSION

We have presented a mathematical model for a single auditory channel in the inner ear. It incorporates a tuned-filter response, a nonlinear receptor response, Poisson con-

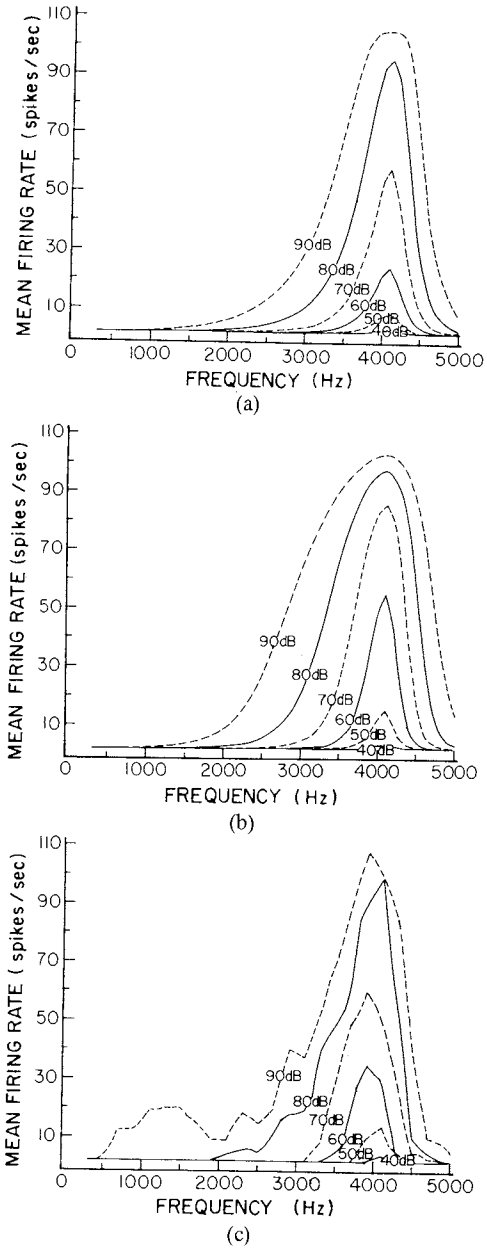

Fig. 4. Mean response of a single afferent fiber to a tone of variable frequency and intensity. (a) The ELFRM results using the exponential receptor saturation function. (b) Results were calculated using the logarithmic function. (c) Data collected by Rose *et al.* [8] are shown for a fiber with a characteristic frequency of 4100 Hz. (Pertinent parameter values are listed in Table I.)

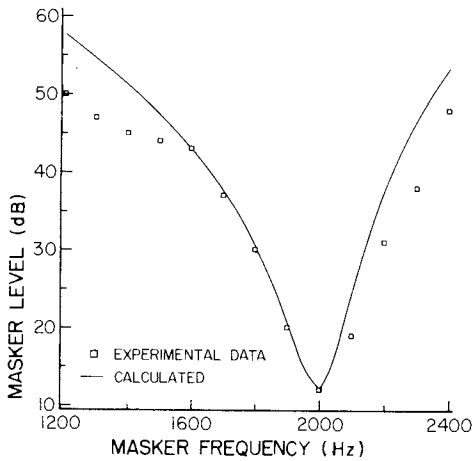

Fig. 5. Human psychophysical tuning curve obtained in a simultaneous masking paradigm. Experimental data (open squares) collected by Johnson-Davies and Patterson [1] for listener DJD. The ELFRM predictions, plotted as the solid curve, utilized a double-tuned filter ($N = 2$) on the low-frequency side, a quadruple-tuned filter ($N = 4$) on the high-frequency side, and a (single-tuned) value of $Q = 8.6$.

version, refractoriness modification, and spontaneous activity. Calculations based on the model are in accord with a variety of physiological and psychophysical data. An encouraging feature is the consistency in the parameter values for all cases. Most of the parameters (R_o, R_m or R_M, θ or α, and γ) are determined directly from the neurophysiological data. τ and R_m are tied to R_M through the parameter γ. A single value for the tuning parameter Q, though free, fits two sets of experimental isointensity contours (CF = 2100 Hz, CF = 4100 Hz) for the squirrel monkey. A nearby value fits a human psychophysical tuning curve. N appears to remain fixed at 2 below CF, and 4 above CF. We have also been able to obtain satisfactory and consistent fits for $N = 1.5/N = 3.0$ using a substantially larger value of Q ($\simeq 90$). This might correspond, for example, to a cascade of single-tuned energy transduction and single-tuned pressure transduction.

Perhaps the least constrained parameter in our model is E_R, the reference or threshold energy, It was varied until the location and magnitude of each peak response in a data set were simultaneously matched. It is of interest to note the rather radical differences in the values of E_R used to match the 2100 Hz and 4100 Hz data (see Table I). In both cases, the optimal magnitude of E_R for the 4100 Hz data was at least two orders of magnitude (20 dB) greater than that for the 2100 Hz data. It is likely that the middle-ear transfer function is an important factor in the decrease of sensitivity at the higher frequency.

In the LFRM model presented in [10], [4], and [11], refractoriness was the sole means of achieving the saturation of the afferent fiber's response, and we indicated that the inclusion of an explicit receptor saturation function would free the model from this restriction. The results presented in this paper (Figs. 2–4) incorporate both saturation and refractoriness. As a matter of interest, we examined the consequences of allowing only saturation to limit the neural count, by excluding the effects of dead time. The result was theoretical isointensity curves, narrower than those presented in Figs. 3 and 4 despite the effects of spread of excitation. In any case, dead time (or an effect like it) should be included in a proper Poisson-based model to produce a count variance less than the count mean ($\gamma > 1$), in accordance with the experiment. It is interesting to note, furthermore, that dead time is a feedback mechanism and, as such, behaves like an automatic gain control (AGC), which is often considered to be an important part of signal processing in the auditory system. Indeed, (3) displays the same form as the classic expression for gain with feedback.

APPENDIX

THE LOGARITHMIC SATURATION FUNCTION

The logarithmic saturation function (6) has been designed to satisfy the following conditions after refractoriness modification: a) Weber's intensity-discrimination law is obeyed for each channel at large stimulus energies; b) a mean-to-variance ratio for the channel count that is fixed and > 1 at large stimulus energies; and c) ability to fit single-fiber neural firing-rate data. The effects of dead time are parametrically included in the function through the parameter R_m (which is related to R_M through (29)), since it was assumed at the outset that the effects of dead time would be incorporated into the final results. We demonstrate these properties in the following.

For calculating intensity discrimination, it is customary to define a detection distance h given by (see [10])

$$h = \frac{[\bar{n}_c(E_o + \Delta E_o) - \bar{n}_c(E_o)]}{[\sigma_c^2(E_o + \Delta E_o) + \sigma_c^2(E_o)]^{1/2}}. \tag{13}$$

Here $\bar{n}_c$ and σ_c^2 are the dead-time-modified count mean and variance, respectively, and E_o is the energy or intensity level. Equation (13) can be approximated as

$$h \simeq \frac{(d\bar{n}_c/dE_o)\Delta E_o}{\sqrt{2}\,\sigma_c}, \tag{14}$$

under the reasonable assumption that the count variance is unchanged between the levels E_o and $E_o + \Delta E_o$.

Rewriting (3) and (4), we obtain

$$\bar{n}_c(f_o) = \lambda(E_o)T/[1 + \lambda(E_o)\tau] \tag{15}$$

and

$$\sigma_c^2(f_o) = \lambda(E_o)T/[1 + \lambda(E_o)\tau]^3, \tag{16}$$

where the rate $\lambda(E_o)$ is given by

$$\lambda(E_o) = \bar{n}_u(f_o)/T. \tag{17}$$

We now form the derivative of (15) with respect to E_o, which leads to

$$\frac{d[\bar{n}_c(f_o)]}{dE_o} = T \cdot \frac{d\lambda(E_o)/dE_o}{[1 + \tau\lambda(E_o)]^2}, \tag{18}$$

so that

$$h \simeq \frac{\Delta E_o}{\sqrt{2}} \frac{d[\bar{n}_c(f_o)]/dE_o}{\sigma_c} = \frac{T\Delta E_o}{\sqrt{2}} \cdot \frac{d\lambda(E_o)/dE_o}{\{T\lambda(E_o)[1 + \tau\lambda(E_o)]\}^{1/2}}. \tag{19}$$

We use the saturation function described in (6),

$$\lambda(E_o) = \frac{c\ln(1 + \beta E_o)}{1 + b\ln(1 + \beta E_o)}, \tag{20}$$

where the additive spontaneous contribution R_o has been omitted for simplicity, and where

$$c = \alpha(R_m - R_o), \tag{21}$$

$$\beta = 1/E_R, \tag{22}$$

$$b = \alpha(R_m - R_o)/(R_M - R_o) = c/(R_M - R_o). \tag{23}$$

Calculating the derivative of (20), and inserting it into (19) gives

$$h \simeq \frac{\beta(Tc)^{1/2}\Delta E_o}{\sqrt{2}(1 + \beta E_o)[1 + b\ln(1 + \beta E_o)][\ln(1 + \beta E_o)]\left[b + c\tau + \{\ln(1 + \beta E_o)\}^{-1}\right]^{1/2}}. \tag{24}$$

In the limit of large stimulus intensities ($\beta E_o \gg 1$), (24) approaches the asymptotic form

$$h \sim \left(\frac{k}{[\ln(\beta E_o)]^2}\right)\frac{\Delta E_o}{E_o} \sim k'\frac{\Delta E_o}{E_o}, \tag{25}$$

where k and k' are constants that are essentially independent of E_o, since the behavior of the denominator of (25) is dominated by E_o. The same result is obtained when the additive spontaneous contribution R_o (see (6)) is included in the calculation. For a fixed detection distance h, (25) corresponds to Weber's intensity-discrimination law.

The count mean-to-variance ratio $\gamma_{\ln}$ is, from (6), (7), (17) and (20),

$$\gamma_{\ln} = [1 + \lambda(E_o)\tau]^2 = \left[1 + R_o\tau + \frac{\tau c\ln(1 + \beta E_o)}{1 + b\ln(1 + \beta E_o)}\right]^2. \tag{26}$$

For large stimulus energies, $\gamma_{\ln} \to [1 + R_o\tau + \tau c/b]^2$, so that

$$\gamma_{\ln} \simeq [1 + \tau R_M]^2, \tag{27}$$

and

$$\tau = (\sqrt{\gamma} - 1)/R_M. \tag{28}$$

It is clear that $\gamma_{\ln}$ is fixed and > 1. Equations (27) and (28) are the same as (9) and (10) for $\gamma_{\exp}$. In this same limit [$\lambda(E_o \to \infty) = R_M$], (A3) provides $\bar{n}_c(f_o) = R_M T/(1 + R_M\tau)$. Using this, and the fact that the dead-time-modified mean count $R_m T \equiv \bar{n}_c(f_o)$, with τ given by (28), establishes the relation between R_M (maximum firing rate before refractoriness modification) and R_m (maximum firing rate after refractoriness modification):

$$R_M = \sqrt{\gamma}\,R_m. \tag{29}$$

Equation (29) is valid for both the logarithmic and the exponential saturation functions.

Finally, we observe that the form of the dead-time-modified logarithmic saturation function is appropriate for fitting single-fiber neural firing-rate data, as demonstrated in Section III-B.

REFERENCES

[1] D. Johnson-Davies and R. D. Patterson, "Psychophysical tuning curves: Restricting the listening band to the signal region," *J. Acoust. Soc. Amer.*, vol. 65, pp. 765–770, 1979.

[2] N. Y. S. Kiang, "A survey of recent developments in the study of auditory physiology," *Ann. Otol. Rhinol. Laryngol.*, vol. 77, pp. 656–675, 1968.
[3] G. Lachs, R. A. Saia, and M. C. Teich, "A neural-counting model incorporating refractoriness and spread of excitation: Extension of the model to include receptor saturation and spontaneous neural activity," *J. Acoust. Soc. Amer.*, vol. 71, p. S18, 1982.
[4] G. Lachs and M. C. Teich, "A neural-counting model incorporating refractoriness and spread of excitation. II. Application to loudness estimation," *J. Acoust. Soc. Amer.*, vol. 69, pp. 774–782, 1981.
[5] M. C. Liberman, "Auditory-nerve response from cats raised in a low-noise chamber," *J. Acoust. Soc. Amer.*, vol. 63, pp. 442–455, 1978.
[6] _____, "Single-neuron labeling in the cat auditory nerve," *Science*, vol. 216, pp. 1239–1241, 1982.
[7] W. J. McGill, "Neural counting mechanisms and energy detection in audition," *J. Math. Psychol.*, vol. 4, pp. 351–376, 1967.
[8] J. E. Rose, J. E. Hind, D. J. Anderson, and J. F. Brugge, "Some effects of stimulus intensity on response of auditory nerve fibers in the squirrel monkey," *J. Neurophysiol.*, vol. 34, pp. 685–699, 1971.
[9] M. C. Teich and S. M. Khanna, "Pulse-number distribution for the neural discharge in the cat's auditory nerve," *J. Acoust. Soc. Amer.*, vol. 71, p. S17, 1982.
[10] M. C. Teich and G. Lachs, "A neural-counting model incorporating refractoriness and spread of excitation. I. Application to intensity discrimination," *J. Acoust. Soc. Amer.*, vol. 66, pp. 1738–1749, 1979.
[11] _____, "A neural-counting model incorporating refractoriness and spread of excitation. III. Application to intensity discrimination and loudness estimation for variable-bandwidth noise stimuli," *Acustica*, in press.
[12] M. C. Teich, G. Lachs, and R. A. Saia, "A neural-counting model based on physiological characteristics of the peripheral auditory system. V. Application to intensity discrimination, loudness estimation, and loudness summation," in preparation.
[13] M. C. Teich, L. Matin, and B. I. Cantor, "Refractoriness in the maintained discharge of the cat's retinal ganglion cell," *J. Opt. Soc. Amer.*, vol. 68, pp. 386–402, 1978.
[14] E. Zwicker, "On a psychoacoustical equivalent of tuning curves," in *Facts and Models in Hearing*, E. Zwicker and E. Terhardt, Eds. Heidelberg: Springer-Verlag, 1974, pp. 132–141.
[15] J. J. Zwislocki, "On intensity characteristics of sensory receptors: A generalized function," *Kybernetik*, vol. 12, pp. 169–183, 1973.

0018-9472/83/0900-0972$01.00